Strand-Separating Activity of Hepatitis C Virus Helicase in the Absence of ATP

David J. T. Porter and Frank Preugschat*

Glaxo Wellcome, 5 Moore Drive, Research Triangle Park, North Carolina 27709

Received October 13, 1999; Revised Manuscript Received January 6, 2000

ABSTRACT: HCV helicase [E(wt)] catalyzed strand separation of a short DNA duplex (F21:HF31) formed from a 5′-hexachlorofluorescein-tagged 31-mer (HF31) and a 3′-fluorescein-tagged 21-mer (F21) complementary to the 5′-end of HF31. Strand separation was monitored by the fluorescence increase associated with the formation of F21 from F21:HF31. In the presence of ATP, the strand-separating activity was catalytic. In the absence of ATP and with E(wt) concentrations greater than that of F21:HF31, a biphasic fluorescence increase was observed at 25 °C. The late phase of this reaction was assigned to the separation of F21 from F21:HF31. The ATP-independent strand-separating reaction occurred more rapidly in the absence of Mg^{2+} than in its presence. This result correlated with a lower T_m value of F21:HF31 in the absence of 3.5 mM Mg^{2+} than in its presence (45 vs 63 °C). The stoichiometry for the strand-separating reaction in the absence of ATP was 8 mol of E(wt) per mole of F21:HF31 separated into single-stranded F21 and HF31. The dissociation constants of HCV helicase for F21, HF31, and F21:HF31 in the absence of Mg^{2+} were 0.6 ± 0.4, 6 ± 1, and 7.3 ± 0.9 nM, respectively. Histidinyl-tagged E(wt) [hE(wt)] and a mutant enzyme [hE(V432A)] were prepared. hE(wt) and E(wt) bound F21 and HF31 with similar affinities and had similar ATP-dependent helicase activities, whereas hE(V432A) bound F21 and HF31 with affinities similar to that of E(wt) but had greatly reduced ATP-dependent helicase activities. In contrast to E(wt) and hE(wt), hE(V432A) did not support the ATP-independent strand-separating reaction. Consequently, the ATP-independent strand-separating reaction was not only the result of the high affinity of the enzyme for single-stranded DNA. The enzyme preferentially used duplex DNA with a 3′-tail for the ATP-dependent helicase reaction. In contrast, the enzyme strand-separated blunt-ended, 5′-tailed, and 3′-tailed duplex DNA equally effectively in the ATP-independent strand-separating reaction.

Helicases are ubiquitous enzymes required for cellular repair, recombination, and replication (*1*, *2*). Our interest in helicases is based on the observation that the HCV[1] genome encodes a unique helicase within the NS3 protein. Because approximately 1% of the population is infected with HCV and available therapies are effective for only a small subpopulation of these patients, an urgent medical need exists for an effective anti-HCV agent (*3*−*5*). Consequently, HCV helicase is an attractive target for development of an antiviral agent for HCV infection.

Even though helicase activity was identified and the associated protein was purified more than 20 years ago (*6*) and numerous crystal structures of helicases under various conditions have been reported (*7*−*10*), the kinetic and chemical mechanism for this class of enzymes is incompletely understood (*2*). Consequently, we have initiated a program to characterize the kinetic and chemical mechanism of ATPase activity and strand-separating activity of the HCV helicase domain isolated from HCV genotype 1b [which is a major subtype found in both Japanese and American populations (*11*)]. The kinetic mechanism of the nucleic acid-stimulated ATPase activity associated with this protein has been reported (*12*). In summary, $(dU)_{18}$ stimulated the rate of ATP hydrolysis more than 27-fold. The binding of $(dU)_{18}$ to the enzyme is associated with a large change in the intrinsic protein fluorescence. Using these changes to monitor the reaction of the enzyme with $(dU)_{18}$, the association rate constant for association of the enzyme with $(dU)_{18}$ was observed to be 50-fold greater in the absence of ATP than in its presence, whereas the dissociation rate constant for dissociation of of E·$(dU)_{18}$ was not affected by ATP. Recently, we have extended our understanding of the kinetic mechanism of the helicase activity of this protein by analysis of the ATP-dependent helicase reaction with a fluorescently tagged duplex oligomer with a defined sequence (*13*). In summary, HCV helicase was active as a monomeric protein that suggested a passive kinetic mechanism (*2*). Furthermore, the enzyme was catalytic in the ATP-dependent helicase assay in which dissociation of single-stranded DNA from the enzyme was the major contributor to k_{cat}.

* To whom correspondence should be addressed. Telephone: (919) 483-9423. Fax: (919) 483-3895. E-mail: fp41724@glaxowellcome.com.

[1] Abbreviations: HCV, hepatitis C virus; E(wt), HCV helicase-truncated domain of the NS3 protein, including amino acid residues 1193−1657 of the HCV genotype 1b polyprotein; hE(wt), truncated domain of the NS3 protein, including amino acid residues 1207−1657 of the HCV genotype 1b polyprotein with six histidinyl residues and a thrombin cleavage site on the amino terminus; hE(V432A), hE(wt) with V432 replaced with an alaninyl residue; E(wt)·ATP, complex between E(wt) and ATP; E(wt)·ATP·NA, complex among E(wt), ATP, and NA where NA is F21, HF31, or F21:HF31; MOPS, 3-(*N*-morpholino)-propanesulfonic acid; Tris, tris(hydroxymethyl)aminomethane; F, chemically modified fluorescein as defined in the Oligos Etc. catalogue; HF, chemically modified hexachlorofluorescein as defined in the Oligos Etc. catalogue; 21-mer, GAG TCA CGA CGT TGT AAA AAA; F21, GAG TCA CGA CGT TGT AAA AAA-F; HF31, HF-TTT TTT ACA ACG TCG TGA CTC TCT CTC TCT C; HF21′, HF-TTT TTT ACA ACG TCG TGA CTC; F31′, C TCT CTC TCT GAG TCA CGA CGT TGT AAA AAA-F; F21:HF31, HF21′:F31′, and F21′:HF21′, duplexes formed from the respective annealing oligomers.

10.1021/bi992384f CCC: $19.00 © 2000 American Chemical Society
Published on Web 04/07/2000

Helicases frequently bind single-stranded nucleic acids with high affinity. By analogy with other single-stranded binding proteins such eukaryotic replication protein A (*14*), adenovirus DNA binding protein (*14*), herpes simplex virus type 1 ICP8 protein (*15*), and T4gp32 (*16*) that catalyze an ATP-independent strand separation of duplex DNA, it was possible that HCV helicase could support an ATP-independent strand-separating reaction. The results herein demonstrated that HCV helicase supports an ATP-independent strand-separating reaction. This reaction was stoichiometric and not catalytic.

EXPERIMENTAL PROCEDURES

Materials. MOPS, Tris, and ammonium sulfate were from Sigma Chemical Co. ATP, poly(rU), and single-stranded DNA cellulose resin were from Pharmacia Biotech. All oligomers with defined sequences were purchased from Oligo Therapeutics, Inc., and were purified by electrophoresis through a 6 M urea−20% polyacrylamide gel.

General Methods. The standard buffer was 0.05 M MOPS (Na^+) at pH 7.0. The standard temperature was 25 °C. Fluorescence data were collected with a Perkin-Elmer LS50B or a Kontron SFM 25 spectrofluorometer. F21 fluorescence was monitored with $\lambda_{ex} = 492$ nm and $\lambda_{em} = 522$ nm; HF31 fluorescence was monitored with $\lambda_{ex} = 538$ nm and $\lambda_{em} = 552$ nm with a 2 mm slit. Fluorescence of F21 that was enzymatically generated from F21:HF31 was monitored with $\lambda_{ex} = 492$ nm and $\lambda_{em} = 522$ nm. In these experiments, the fractional fluorescence of F21:HF31 at $\lambda_{ex} = 492$ nm and $\lambda_{em} = 522$ nm was assigned a value of 0.2. Fluorescence time courses that are presented are representative of at least two independent experiments. The differences between experimental tracings were less than 10%. Absorbance and conventional kinetic data were obtained from a UVIKON 860 spectrophotometer. Equations described below were fitted to the data by a nonlinear least-squares method using SigmaPlot from Jandel Scientific (Corte Madera, CA).

Preparation of HCV Helicase. The helicase domain of HCV helicase (E) was purified as described previously (*12*). The histidinyl-tagged helicase domain [hE(wt)] and hE-(V432A) were purified as described previously (*23*). The concentrations of E(wt) and hE(wt) were estimated spectrophotometrically using an ϵ_{280} of 88.5 mM^{-1} cm^{-1}, which is based on dU_{18} binding sites (*12*). The concentration of hE-(V432A) was determined by titration of the enzyme with F21.

Assay of HCV Helicase Activities. Strand separation of F21:HF31, where a 21-mer and a complementary 31-mer were modified with fluoresceinyl and hexachlorofluoresceinyl moieties on the 3′-end (F21) and 5′-end (HF31), respectively, was assayed spectrofluorometrically ($\lambda_{ex} = 492$ nm and $\lambda_{em} = 522$ nm) as described previously (*13*). Typically, the extent of fluorescence enhancement observed upon strand separation was 5−9-fold. This method is based on the fluorescence resonance energy transfer method of Bjornson et al. (*17*).

Analysis of Titration Data. Titration of HCV helicase with nucleic acid was monitored spectrofluorometrically. Because the dissociation constant for dissociation of the nucleic acid for the enzyme was comparable to the concentration of the nucleic acid being titrated, the quadratic equation describing the binding of ligand to receptor was fitted to the data (eq 1).

$$F = 1 + \Delta F_\infty \left(\frac{[NA_t] + [E_t] + K_d}{2[NA_t]} - \frac{1}{2[NA_t]} \sqrt{([NA_t] + [E_t] + K_d)^2 - 4[E_t][NA_t]} \right) \quad (1)$$

where K_d is the dissociation constant for dissociation of the enzyme from the nucleic acid, $[NA_t]$ is the nucleic acid concentration, and $[E_t]$ is the enzyme concentration.

Titration of the ATP-independent strand separation of F21:HF31 with HCV helicase is described by eqs 2a and 2b

$$F([E]) = F_0 + \frac{F_\infty - F_0}{[E_s]}[E] \qquad [E] \le [E_s] \quad (2a)$$

$$F([E]) = F_\infty \qquad [E] > [E_s] \quad (2b)$$

where $[E_s]$ is the concentration of E yielding complete strand separation. The initial fluorescence of F21:HF31 (F_0) in the absence of enzyme was adjusted to 0.2.

Preparation of F21:HF31. Stock solutions of F21:HF31 (5 μM) in the standard buffer with 3.5 mM $MgCl_2$ were prepared by heating a solution of 5 μM F21 and 5 μM HF31 to 90 °C for 3 min and then cooling to room temperature over several hours. The annealing of F21 with HF31 could be monitored by the associated fluorescence quenching of F21 ($\lambda_{ex} = 492$ nm and $\lambda_{em} = 522$ nm) upon formation of F21:HF31. In the presence of excess HF31, the fluorescence of F21 was quenched 90%. Consequently, the maximal extent of fluorescence enhancement upon strand separation was expected to be approximately 10-fold. Experimentally, this value varied between 5- and 9-fold. This difference was attributed to experimental error in preparing the solutions of F21 and HF31 for the annealing reaction. For example, a 10% excess of F21 in the annealing reaction would result in a 50% decrease in the observed extent of fluorescence enhancement upon strand separation of F21:HF31. The same substrate preparation of F21:HF31 was used for generation of the data for each individual figure, whereas the data for different figures were collected with different preparations of F21:HF31. As a result, the apparent extent of enhancement of F21 fluorescence upon strand separation varied between figures. This variation was attributed to variations in the amount of single-stranded F21 in our preparations of F21:HF31.

Determination of T_m Values. The T_m values of 500 nM F21:HF31 and 21:31 were determined with a Gilford response spectrophotometer. The standard buffer was supplemented with either 1.0 mM EDTA or 3.5 mM $MgCl_2$. The reaction was monitored at 260 nm as the temperature was either increased from 30 to 90 °C or decreased from 90 to 30 °C at a rate of 0.5 °C min^{-1}. The T_m value was the average of the inflection points of the melting and annealing curves.

Determination of the Value of the Bimolecular Rate Constant for Annealing of F21 with HF31. Annealing of F21 with HF31 was associated with a 90% quenching of the fluorescence of F21 (with $\lambda_{ex} = 492$ nm and $\lambda_{em} = 522$ nm). This signal change was used to monitor the reaction of F21 with HF31. The quenching of F21 fluorescence by excess

HF31 was first-order in F21 concentration. Equation 3 was fitted to these data to yield a pseudo first-order rate constant (k_{obs}) for the reaction

$$F(t) = F_\infty + \Delta F e^{-k_{obs}t} \quad (3)$$

where $F(t)$ is the fluorescence at time t, ΔF is the maximal fluorescence change, and F_∞ is the fluorescence at the end of the reaction.

Values for the pseudo-first-order rate constant for the quenching of 10 nM F21 by 20, 40, 60, 80, and 100 nM HF31 were determined for the standard buffer supplemented with 3.5 mM $MgCl_2$. The value of the bimolecular rate constant (k_2) was calculated from the slope of the linear dependence of k_{obs} on HF31 concentration (eq 4).

$$k_{obs}([HF31]) = k_2[HF31] \quad (4)$$

Annealing of F21 generated from the enzymatic strand separation of F21:HF31 was monitored under experimental conditions in which the concentrations of F21 and HF31 were equal (second-order conditions) or the concentration of HF31 was greater than the concentration of F21 (pseudo-first-order conditions). In the former case, the enzymatic reaction was quenched with poly(rU) in the absence of added HF31. With these experimental conditions, the disappearance of F21 was a second-order process described by eq 5

$$[F21(t)] = \frac{[F21]_0}{1 + k_2 t[F21]_0} \quad (5)$$

where $[F21(t)]$ is the concentration of F21 at time t, k_2 is the bimolecular rate constant, and $[F21]_0$ is the concentration of F21 after addition of the quenching reagent to the enzymatic reaction.

The concentrations of F21(t) were calculated from the fluorescence data with eq 6

$$[F21(t)] = \frac{F(t) - F_0}{F_\infty - F_0}[F21{:}HF31]_0 \quad (6)$$

where $F(t)$ is the fluorescence of the solution at time t, F_0 is the fluorescence at time zero, and F_∞ is the fluorescence after complete strand separation.

When the enzymatic reaction was quenched with poly(rU) in the presence of excess HF31, the fluorescence of enzymatically generated F21 was quenched in a first-order process. Equation 3 was fitted to these data to give a pseudo-first-order rate constant for the process. The bimolecular rate constant for the annealing process was calculated with eq 4.

Time Courses for Fluorescence Changes during the Reaction of the Enzyme with F21:HF31. The time course for the enhancement of F21:HF31 fluorescence upon addition of enzyme ([E] ≫ [F21:HF31]) and ATP was a monophasic process described by eq 3. In contrast, the time course for the enhancement of F21:HF31 fluorescence upon addition of the enzyme in the absence of ATP was a biphasic process described by eq 7.

$$F(t) = F_\infty + \Delta F_1 e^{-k_1 t} + \Delta F_2 e^{-k_2 t} \quad (7)$$

where ΔF_1 and ΔF_2 are the fluorescence changes associated with the early and late phases of the reaction, respectively, k_1 and k_2 are the corresponding first-order rate constants, and F_∞ is the fluorescence at the end of the reaction.

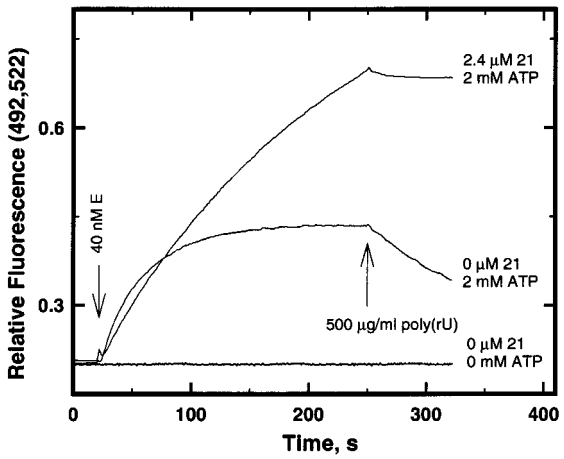

FIGURE 1: Strand separation of F21:HF31 by substoichiometric amounts of E(wt) in the presence of ATP. The relative fluorescence of a solution of 400 nM F21:HF31 in the standard buffer with 3.5 mM $MgCl_2$ and the indicated concentrations of ATP and 21 was adjusted to 0.2 (λ_{ex} = 492 nm and λ_{em} = 522 nm). The strand-separating reactions were initiated by the addition of 40 nM E(wt) at 25 s. The enzymatic reaction was quenched with 500 μg/mL poly(rU) at 250 s.

RESULTS

Strand Separation of F21:HF31 at Substoichiometric Ratios of E(wt) to F21:HF31. Strand separation of duplex F21:HF31 is associated with a 5−9-fold increase in the fluorescence of F21 (λ_{ex} = 492 nm, λ_{em} = 522 nm) that can be used to monitor the HCV helicase reaction (*13*). Examples of the reaction of 40 nM E with 400 nM F21:HF31 are presented in Figure 1. Under these conditions, E(wt) supported strand separation of F21:HF31 in the presence of ATP (eq 8a), but did not support strand separation in the absence of ATP.

$$F21{:}HF31 + ATP \xrightarrow{E} F21 + HF31 + ADP + P_i \quad (8a)$$

$$21{:}HF31 + ATP \xrightarrow{E} 21 + HF31 + ADP + P_i \quad (8b)$$

$$F21 + HF31 \rightarrow F21{:}HF31 \quad (8c)$$

$$21 + HF31 \rightarrow 21{:}HF31 \quad (8d)$$

$$E + poly(rU) \rightleftharpoons E{\cdot}poly(rU) \quad (8e)$$

However, in the absence of a trap for HF31 or F21, the steady-state fluorescence value corresponded to that expected for only 20% strand separation (Figure 1, middle trace). Inhibition of the enzyme in this reaction with 500 μg/mL poly(rU) at 250 s resulted in a time-dependent decrease in the fluorescence of the solution. The value of the bimolecular rate constant describing the quenching data was $(1.30 \pm 0.01) \times 10^5$ M^{-1} s^{-1} (eq 8e). Under similar conditions, the value of the bimolecular rate constant for annealing authentic F21 with HF31 (eq 8c) was $(2.62 \pm 0.04) \times 10^5$ M^{-1} s^{-1}. The similarity of these values suggested that the quenching of the fluorescence observed in the inhibited enzymatic reaction was the result of annealing of fully separated F21 and HF31. Consequently, the plateau value for the fluorescence in the lower tracing of Figure 1 was the steady-state concentration

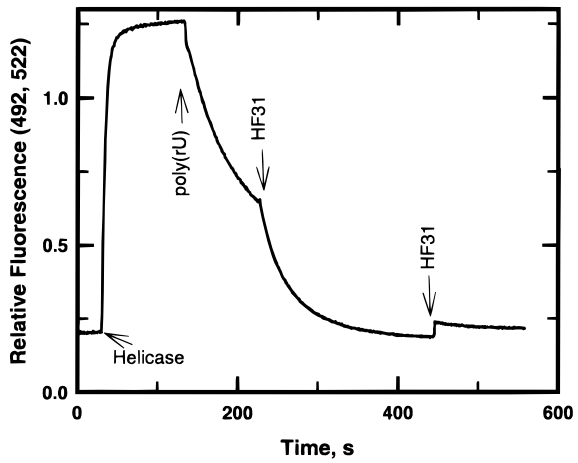

FIGURE 2: Strand separation of F21:HF31 by high concentrations of E(wt) in the presence of ATP. Strand separation of 50 nM F21:HF31 in the presence of 2 mM Mg^{2+}ATP and 3.5 mM Mg^{2+} was monitored as described in the legend of Figure 1. The reaction was initiated at 25 s by the addition of 477 nM E(wt). The enzymatic reaction was quenched at 140 s with 500 μg/mL poly(rU). The single-stranded F21 that was generated was annealed to HF31 by addition of excess HF31 (100 nM).

of free F21 for which the rate of enzymatic strand separation was equal to the rate of nonenzymatic annealing. On the basis of this interpretation, the extent of strand separation of F21:HF31 could be increased by the addition of a trap for HF31 that would effectively eliminate the annealing of F21 with HF31. The oligomer 21, which had the same sequence as F21 but lacked the fluoresceinyl moiety, is an efficient trap for HF31 (eq 8d). Even though the initial velocity of the strand-separating reaction in the presence of 2.4 μM 21 was lower than that in its absence due to the binding of E(wt)·ATP to 21 ($K_d = 210 \pm 20$ nM), the enzymatically dependent increase in fluorescence approached a value (>1) that was expected for complete strand separation (data not shown). Furthermore, inhibition of the enzymatic activity in the presence of 21 with poly(rU) did not result in a fluorescence decrease (Figure 1, upper trace). Thus, enzymatically generated HF31 was effectively removed from solution by annealing with the excess 21 (eq 8d) such that the fluorescence of F21 was not quenched by annealing with HF31 after inhibition of the enzymatic activity with poly(rU). These results demonstrated that the fluorescence quenching observed upon inhibition of E(wt) during the reaction with F21:HF31 was the result of annealing of enzymatically generated F21 with HF31 (eq 8c).

In the example of the strand-separating reaction presented in Figure 1, 40 nM E(wt) catalyzed the strand separation of 160 nM F21:HF31 prior to addition of poly(rU) (upper trace of Figure 1) in the presence of ATP. Thus, the enzyme was functioning as a catalyst and not as a reactant.

Strand Separation of F21:HF31 at High Ratios of E(wt) to F21:HF31 in the Presence of ATP. Strand separation of F21:HF31 by E(wt) and ATP in the absence of the trapping agent 21 was incomplete (Figure 1). However, the fluorescence of a solution of 50 nM F21:HF31 and 2 mM ATP could be driven to that expected for complete strand separation with 477 nM E(wt) (Figure 2). The increase in fluorescence was essentially a monophasic process (eq 3) with a k_{obs} of 0.209 ± 0.004 s^{-1}. The observed fluorescence change when [E(wt)] ≫ [F21:HF31] could be attributed to

Table 1: Dissociation Constants of E(wt), hE(wt), and hE(V432A) for F21 and HF31 in the Absence of Mg^{2+} (1.0 mM EDTA)[a]

	E(wt)	hE(wt)	hE(V432A)
F21			
ΔF_∞	0.083 (1)	0.11 (1)	0.08 (1)
K_d (nM)	0.6 (4)	2.0 (7)	0.9 (8)
HF31			
ΔF_∞	−0.626 (8)	−0.63 (1)	−0.57 (1)
K_d (nM)	6 (1)	17 (1)	16 (1)

[a] Parameters are defined by eq 1 in Experimental Procedures. The values in parentheses are the standard error of the least significant figure reported.

separation of the F from the HF moiety by either strand separation or binding of E(wt)·ATP to HF and F moieties. The latter possibility was eliminated by the following experiment. F21, HF31, and F21:HF31 were displaced from E(wt)·ATP by addition of a large excess of poly(rU) (500 μg/mL). If strand separation had not occurred, the fluorescence of the solution should rapidly return to that of F21:HF31 in a process described by a first-order rate constant corresponding to the dissociation of E(wt)·ATP·F21:HF31. The value of this dissociation rate constant is 0.84 s^{-1}, which corresponds to a half-time of 0.82 s (*13*). Because the fluorescence of the resultant solution returned to that of F21:HF31 very slowly (Figure 2), the fluorescence changes observed after inhibition of the enzymatic reaction with poly(rU) could not be attributed to dissociation of E(wt)·ATP·F21:HF31. The fluorescence quenching was attributed to annealing of F21 and HF31 for the following reasons. First, the value of the bimolecular rate constant for the quenching reaction in the absence of added HF31 was determined from these data by eq 5 to be $(2.93 \pm 0.04) \times 10^5$ M^{-1} s^{-1}. Second, the rate of fluorescence quenching was enhanced by the addition of 100 nM HF31. Under these conditions, the decrease in fluorescence was a first-order process. The value of the pseudo-first-order rate constant for this process was determined by eq 3 to be 0.0244 ± 0.0002 s^{-1}. This corresponded to a bimolecular rate constant of $(2.44 \pm 0.02) \times 10^5$ M^{-1} s^{-1} (eq 4). Both of these values for the bimolecular rate constant were in good agreement with the independently determined value for the annealing of F21 with HF31 [$(2.62 \pm 0.04) \times 10^5$ M^{-1} s^{-1}]. The final fluorescence of the solution was that expected for complete annealing of F21 with HF31. The small burst in fluorescence quenching (~10%) observed immediately after addition of poly(rU) to the enzymatic reaction (Figure 2) was that expected for displacement of F21 from E(wt) by poly(rU) (Table 1).

Strand Separation of F21:HF31 at High Ratios of E(wt) to F21:HF31 in the Absence of ATP. In contrast to the results obtained with substoichiometric ratios of E(wt) to F21:HF31 in the absence of ATP (Figure 1), E(wt) increased the fluorescence of F21:HF31 in the absence of ATP when the enzyme concentration was much greater than the concentration of F21:HF31. Upon addition of 477 nM E(wt) to 50 nM F21:HF31 in the absence of ATP, the solution fluorescence slowly increased to the value expected (~1.4) for complete strand separation (Figure 3A). The time course of the fluorescence increase was biphasic (eq 7) with values for the first-order rate constants of 0.0340 ± 0.0008 and 0.00126 ± 0.00002 s^{-1} (Figure 3A). The amplitudes of the two phases were -0.583 ± 0.004 and -0.617 ± 0.007,

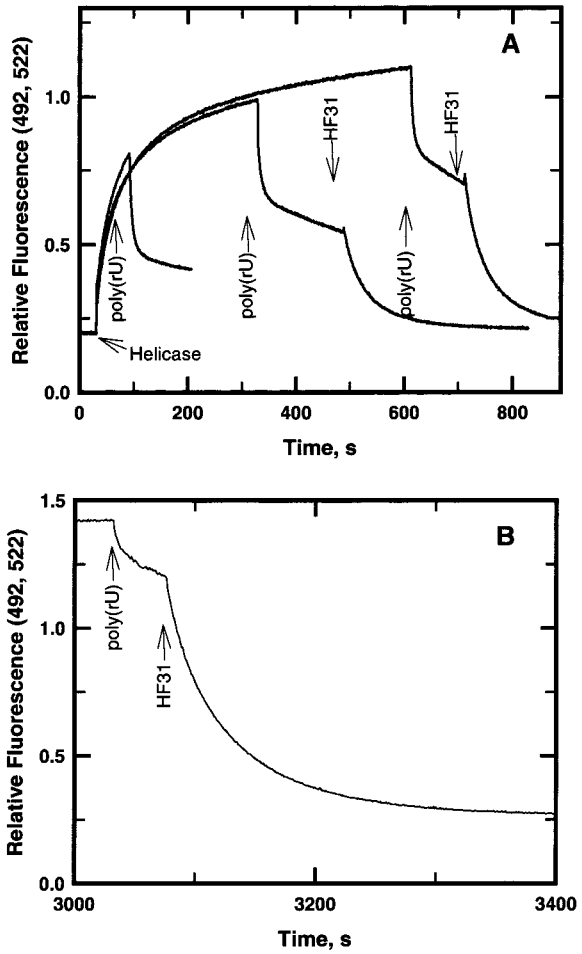

FIGURE 3: Time course for strand separation of F21:HF31 catalyzed by E(wt) in the absence of Mg^{2+}ATP but in the presence of Mg^{2+}. (A) Strand separation of F21:HF31 after selected reaction times. Several strand-separating reactions were initiated at 25 s by the addition of 477 nM E(wt) to 50 nM F21:HF31. The fluorescence change associated with the reaction was monitored with $\lambda_{ex} = 492$ nm and $\lambda_{em} = 522$ nm. At 85, 320, and 590 s, the enzymatic reaction was quenched with 500 μg/mL poly(rU). The single-stranded F21 that was generated was annealed to HF31 by addition of excess HF31 (100 nM). The fraction of the fluorescence change associated with the slow phase of the fluorescence quenching reaction was attributed to free F21. (B) Strand separation of F21:HF31 after incubation of 50 nM F21:HF31 with 477 nM E(wt) for 3000 s. The reaction was quenched with 500 μg/mL poly(rU). HF31 (100 nM) was added to anneal F21 with concomitant quenching of fluorescence.

respectively. Inhibiting the enzymatic reaction after approximately 250 s with 500 μg/mL poly(rU) resulted in a biphasic time course for fluorescence quenching (Figure 3A). The value of the bimolecular rate constant describing the late phase of this reaction (eq 5) was $(2.22 \pm 0.07) \times 10^5$ M^{-1} s^{-1}. The rate of quenching was enhanced by addition of 100 nM HF31 to this solution. The value of the bimolecular rate constant calculated from these data was $(2.22 \pm 0.02) \times 10^5$ M^{-1} s^{-1}. These values for the bimolecular rate constant were in good agreement with that determined for annealing of F21 to HF31 $(2.62 \pm 0.04) \times 10^5$ M^{-1} s^{-1}. Consequently, the late phase of the quenching reaction after addition of poly(rU) to the enzymatic reaction mixture (Figure 3A) was attributed to the annealing of F21 with HF31.

The amplitude of the early phase of the quenching reaction was too large to be attributed solely to dissociation of F21 from E(wt)·F21 as was the case for the ATP-dependent reaction (Figure 2A). The rate of the reaction was sufficiently large that it could be attributed to dissociation of F21:HF31 from E(wt)·F21:HF31. Thus, the data of Figure 3A suggested that approximately 50% of F21:HF31 was separated into F21 and HF31 after a 320 s reaction. The extent of strand separation (amplitude of the final phase of the quenching reaction) increased with increasing time (Figure 3A). After 3000 s (Figure 3B), the amplitude of the final phase of the reaction was very similar to that in which 2 mM ATP was present (compare Figure 2 with Figure 3B). The time course of the amplitude of the late phase of the quenching reaction (taken from panels A and B of Figure 3) was monophasic (eq 3) with a first-order rate constant of 0.0013 ± 0.0004 s^{-1}. Because this value corresponded to the value of the first-order rate constant for the late phase of the enzyme-catalyzed fluorescence increase (Figure 3A), the late phase of the fluorescence increase was equated to strand separation. This interpretation was confirmed by the observation that if the enzymatic reaction was quenched with 2.4 μM 21 instead of poly(rU), the early phase of the reaction was similar to that described above, whereas the late phase of the reaction was eliminated (data not shown). In this experiment, 21 eliminated the annealing of enzymatically generated F21 and HF31 by trapping HF31 (eqs 8c and 8d).

These results demonstrated that 477 nM E(wt) could strand separate 50 nM F21:HF31 as completely in the absence of ATP as in its presence. However, strand separation of 50 nM F21:HF31 by 477 nM E(wt) occurred 200-fold more rapidly in the presence of ATP ($k = 0.209$ s^{-1}) than in its absence ($k = 0.00126$ s^{-1}).

Effect of $MgCl_2$ on Strand Separation of F21:HF31 at High Ratios of E(wt) to F21:HF31 in the Absence of ATP. Previous experiments in which the strand separation of F21:HF31 by E(wt) was monitored included 3.5 mM Mg^{2+} in the standard buffer. Mg^{2+} was included as a cofactor for the ATP-hydrolyzing activity of HCV helicase. Because HCV helicase-dependent strand separation occurred in the absence of ATP, it was of interest to determine if Mg^{2+} was required for the ATP-independent strand-separating reaction. In the presence of 1.0 mM EDTA, which was added to scavenge fortuitous metal in the buffer solutions, E(wt) supported the efficient strand separation of F21:HF31 (Figure 4). The time course of the fluorescence increase was biphasic (Equation 7) with first-order rate constants of 0.121 ± 0.003 and 0.0107 ± 0.0003 s^{-1} (Figure 4). The amplitudes of the early and late phases were -0.731 ± 0.009 and -0.418 ± 0.006, respectively. This value of the rate constant for the late phase of the reaction, which was associated with strand separation (see above), was approximately 10-fold larger than the value determined in the presence of $MgCl_2$. Termination of the enzymatic reaction with 500 μg/mL poly(rU) resulted in a very low rate of fluorescence quenching. This result was consistent with the slow annealing rate of F21 and HF31 observed in the absence of Mg^{2+}. Addition of 3.5 mM Mg^{2+} increased the annealing rate (Figure 4). Subsequent addition of 100 nM HF31 also increased the annealing rate (Figure 4). For comparison, the time course for the strand-separating reaction in the presence of 3.5 mM Mg^{2+} is included. The increased rate of strand separation of F21:HF31 was associ-

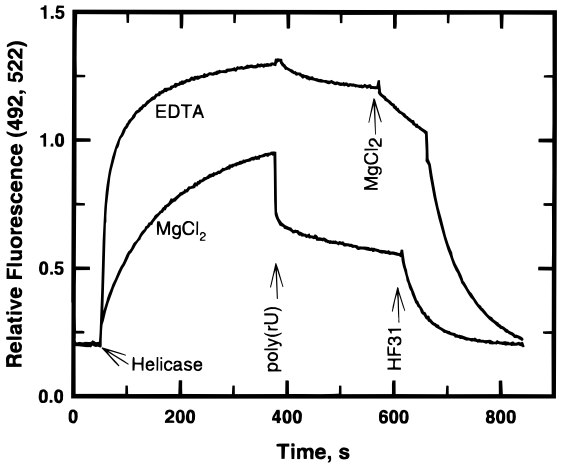

FIGURE 4: Comparison of the strand-separating reaction in the presence of Mg^{2+} to that in the presence of EDTA. E(wt) (477 nM) catalyzed the strand separation of 50 nM F21:HF31 in the presence of 3.5 mM Mg^{2+} (lower trace) or 1.0 mM EDTA (upper trace). The reactions were quenched with 500 μg/mL poly(rU) at 370 s. Excess Mg^{2+} (3.5 mM) was added to the EDTA-containing reaction mixture at 540 s. HF31 (100 nM) was added to both reaction mixtures at 630 s.

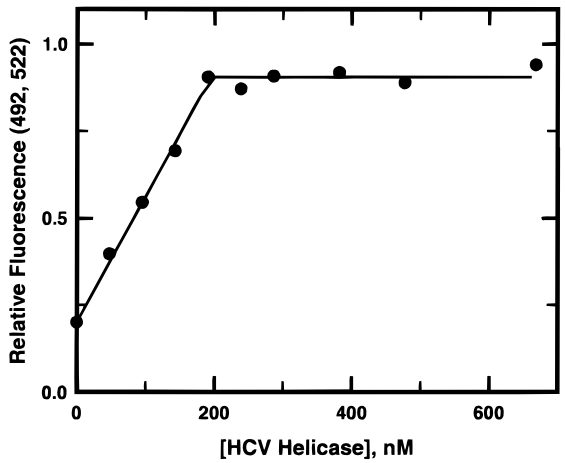

FIGURE 5: Concentration dependence of the extent of strand separation by E(wt). The fluorescence change associated with the reaction of 25 nM F21:HF31 with selected concentrations of E(wt) (1.0 mM EDTA) was determined after the system had attained a steady state (traces analogous to that of the upper trace of Figure 4). The fluorescence at the end of each reaction was normalized to the fluorescence of untreated F21:HF31. The fluorescence of F21:HF31 in the absence of enzyme was set to 0.2. Equation 2 was fitted to these data to give $E_s = 195 \pm 5$ and $F_\infty = 0.90 \pm 0.01$. The solid line was calculated with eq 1 and the values of these parameters.

ated with a lower melting temperature (T_m) for F21:HF31 in the absence of $MgCl_2$. The T_m of 500 nM F21:HF31 in the standard buffer in the presence of 3.5 mM $MgCl_2$ was 63 °C. The value was the same when measured by melting or annealing (rate of temperature change was 0.5 °C/min). In contrast to these results, the melting and annealing curves for F21:HF31 in the standard buffer without $MgCl_2$ exhibited hysteresis. The T_m was 48 °C and the T_m for annealing 41.5 °C. The T_m for 21:31 in the standard buffer was 67 °C.

Stoichiometry of F21:HF31 for E(wt) in the Strand Separation Reaction in the Absence of $MgCl_2$. The extent of ATP-independent strand separation of F21:HF31, measured by the fluorescence increase ($\lambda_{ex} = 492$ nm and $\lambda_{em} = 522$ nm), was determined as a function of enzyme concentration in the standard buffer supplemented with 1.0 mM EDTA. The effect of helicase concentration on the maximal fluorescence increase of 25 nM F21:HF31 [measured 20 min after addition of E(wt) at 22 °C] was determined. The extent of the fluorescence change was linearly dependent on enzyme concentration up to 200 nM E(wt), at which point no further increase in fluorescence was observed with increasing enzyme concentration (Figure 5). Equation 2 was fitted to these data to give a minimal enzyme concentration of 195 $\pm$ 5 nM for completion of the strand-separating reaction in the absence of ATP. The stoichiometry of the reaction [moles of E(wt) per mole of F21:HF31] was calculated from these data to be 7.8.

Affinity of HCV Helicase for F21 and HF31 in the Absence of $MgCl_2$. Titration of HCV helicase by F21 and HF31 in the absence of Mg^{2+} (1.0 mM EDTA) was monitored spectrofluorometrically as described in Experimental Procedures. The dissociation constants of E(wt), hE(wt), and hE(V432A) for F21 and HF31 are summarized in Table 1.

Comparison of the ATP-Independent Strand Separation Activity of E(wt), hE(wt), and hE(V432A). Numerous single-stranded binding proteins have been shown to support stoichiometric strand separation of duplex nucleic acids (*14*−*16*). Consequently, the ATP-independent strand-separating activity of E(wt) could be solely dependent on its single-stranded nucleic acid binding activity. To address this possibility, a mutant of E(wt), hE(V432A), which was tagged with multiple histidinyl residues on the amino terminus for ease of purification, was prepared that had reduced helicase activity. In the standard helicase assay with 2 mM ATP and 50 nM F21:HF31, the initial velocities of strand separation catalyzed by E(wt) and hE(wt) were similar, whereas the initial velocity for hE(V432A) was ~3% of the corresponding value for E(wt) or hE(wt). However, hE(V432A) bound F21 and HF31 with affinities similar to that observed for E(wt) and hE(wt) (Table 1). The time course of the fluorescence increase associated with the ATP-independent strand separation of 25 nM F21:HF31 by 500 nM hE(wt) was biphasic (eq 7) with first-order rate constants of 0.101 $\pm$ 0.004 and 0.0096 $\pm$ 0.0005 s^{-1} (Figure 6). The amplitudes of the early and late phases were -0.93 ± 0.02 and -0.56 ± 0.01, respectively. The values of these parameters for hE(wt) were very similar to those for E(wt) (Figure 4). In contrast, this activity was greatly reduced or absent for hE(V432A). These results demonstrated that the ATP-independent strand-separating activity was not solely dependent on the single-stranded DNA binding activity of HCV helicase.

Strand-Separating Activity of E(wt) in the Absence of ATP with Blunt-Ended Duplex DNA or Duplex DNA with a 5′-Tail. HCV helicase selectively catalyzes the strand separation of duplex nucleic acids with a 3′-tail (3′-polarity) in the presence of ATP (*18*). The experiments we have described for the ATP-independent strand-separating activity of this enzyme were with F21:HF31 which has a 3′-tail. The question arises as to whether HCV helicase also exhibits 3′-polarity in the ATP-independent strand-separating reaction. Thus, the strand-separating activity of the enzyme was examined with a blunt-ended DNA duplex (F21′:HF21′) and a duplex DNA with a 5′-tail (HF21′:F31′). The duplex portion of these potential substrates had the same sequences as the duplex portion of F21:HF31. The fluorescence changes upon formation of HF21′:F31′, HF21′:F21, and F21:HF31

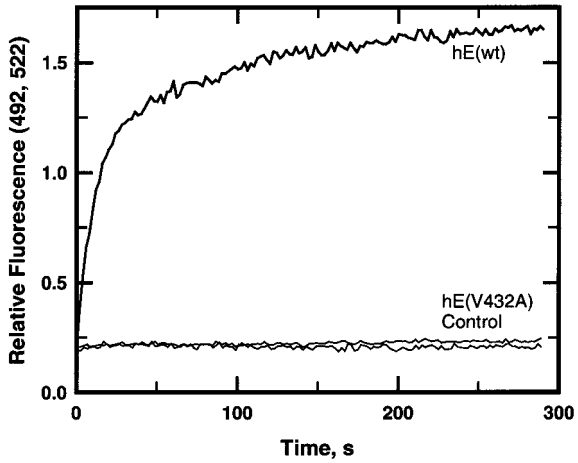

FIGURE 6: Comparison of the strand-separating activity of hE(wt) and hE(V432A). Strand separation of 25 nM F21:HF31 by 500 nM hE(wt) and hE(V432A) in 50 mM MOPS K^+ supplemented with 1.0 mM EDTA Na^+ was monitored as described in the legend of Figure 4. The control sample was 25 nM F21:HF31 in the absence of enzyme.

Table 2: Strand-Separating Activity of 500 nM E(wt), hE(wt), or hE(V432A) with 25 nM F21′:HF21′, HF21′:F31′, or F21:HF31 as Substrates in the Absence of Mg^{2+} (1.0 mM EDTA)[a]

	F21′:HF21′	HF21′:F31′	F21:HF31
E(wt)	0.0157 (2) s^{-1}	0.014 (1) s^{-1}	0.0107 (3) s^{-1}
hE(wt)	0.0144 (2) s^{-1}	0.0073 (4) s^{-1}	0.0096 (5) s^{-1}
hE(V432A)	0.0028 (4) s^{-1}	$<10^{-4}$ s^{-1}	$<10^{-4}$ s^{-1}

[a] Equation 7 was fitted to the time courses for the fluorescence changes with $\lambda_{ex} = 492$ nm and $\lambda_{em} = 522$ nm). The values of the pseudo-first-order rate constant for the late phase of the reaction (k_2), which corresponded to the strand separation reaction, are reported. The values in parentheses are the standard error of the least significant figure reported.

from the respective oligomers were similar. The time courses for the fluorescence increase upon mixing 500 nM enzyme with 25 nM duplex DNA were biphasic. The observed rate constants for the late phase of the reaction, which corresponded to strand separation, are summarized in Table 2. These results suggested that in the absence of ATP, polarity was not important. E(wt) and hE(wt) strand separated 3′- and 5′-tailed duplex DNA and blunt-ended duplex DNA with comparable efficiencies, whereas hE(V432A) did not use these DNA substrates. The 5′-tailed and blunt-ended duplex DNAs were not substrates for any of these enzymes in the ATP-dependent helicase reaction.

DISCUSSION

The role of HCV helicase in the replicative cycle of HCV is most likely the ATP-dependent strand separation of genomic RNA (*19*). In addition to this activity, the enzyme has an ATP-dependent DNA helicase activity (*13*) and a nucleic acid-stimulated ATPase activity (*19*). This work demonstrated that the enzyme also has an ATP-independent strand-separating activity with short duplex DNA as the substrate. Similar ATP-independent strand-separating activity has been observed for eukaryotic replication protein A (*14*), adenovirus DNA binding protein (*14*), herpes simplex virus type 1 ICP8 protein (*15*), and T4gp32 with poly[d(A-T)] as the substrate (*16*). Presumably, the strand-separating activity of these latter proteins is the result of the high affinity of the proteins for single-stranded DNA. hE(V432A) exhibited very low ATP-dependent strand-separating activity but exhibited a high affinity for single-stranded DNA (*23*). Because this mutant did not support ATP-independent strand separation but bound single-stranded DNA with high affinity, single-stranded DNA binding activity was not the major contributor to the ATP-independent strand-separating activity observed for E(wt).

The kinetics for the fluorescence changes associated with the ATP-independent duplex separation were biphasic in the presence or absence of Mg^{2+}. The fluorescence occurring in the late phase of the reaction was associated with strand separation. This was demonstrated by kinetics of fluorescence quenching of F21 after inhibition of the enzymatic reaction with poly(rU). Thus, the bimolecular rate constant for fluorescence quenching under second-order conditions (no HF31 added) and pseudo-first-order conditions (excess HF31 added) was similar to that for the annealing of free HF31 with F21.

The progress of the ATP-independent strand-separating phase of the reaction was 8-fold more rapid in the absence of Mg^{2+} than in its presence. This effect was correlated with an 18 °C decrease in the T_m of F21:HF31 upon removal of Mg^{2+} from the buffer. Thus, a decreased stability of the duplex correlated with an increased rate of strand separation by E(wt). These results suggested that Mg^{2+} was not a necessary participant in the enzymatic separation of F21:HF31 into F21 and HF31. HSV-1 ICP8 (*15*) and replication protein A (*14*) have ATP-independent strand-separating activities such as HCV helicase. Mg^{2+} also potently inhibited these strand-separating activities. If the results for the ATP-independent strand-separating activity of HCV helicase can be extrapolated to the ATP-dependent helicase reaction, then Mg^{2+} may only be needed for the hydrolysis of ATP and the associated reactions coupling ATP hydrolysis to the strand-separating reaction. Thus, the ATP-dependent strand-separating reaction could be envisioned as two half-reactions. The first half-reaction was the separation of base pairs in the nucleic acid duplex and translocation of the duplex coupled to isomerization of the enzyme from a higher-energy state to a lower-energy state. The second half-reaction was the coupling of ATP hydrolysis to return the enzyme to a higher energy state that is capable of another cycle of separation of base pairs. The observation of an ATP-independent strand-separating reaction suggested that the ground state of the enzyme had sufficient energy to separate multiple base pairs.

In the absence of accessory proteins, helicases mediate strand separation either stoichiometrically (multiple helicase molecules per molecule of duplex separated) or catalytically (multiple molecules of duplex separated per helicase molecule). For example, *Escherichia coli* helicase II (UvrD) mediates strand separation stoichiometrically (*20*), whereas RecBCD and T4 dda helicase mediate the reaction catalytically (*21*, *22*). In the absence of ATP, HCV helicase functioned much as UvrD in that both proteins mediate strand separation stoichiometrically. However, ATP was required to raise the ground state of UvrD to a state with strand-separating potential, whereas ATP was not required for HCV helicase to facilitate this reaction stoichiometrically.

The stoichiometry of the ATP-independent strand-separating reaction was 8 mol of enzyme per mole of F21:HF31.

Because F21:HF31 had 21 base pairs, this stoichiometry suggested that each mole of enzyme had sufficient energy to separate 2.5 mol of base pairs. Whether or not the similarity of this value to the number of base pairs (approximately 2) separated during a single cycle of the ATP-dependent helicase reaction in which presumably one molecule of ATP is hydrolyzed (*13*) is mechanistically significant or only fortuitous is unclear. The site size of E(wt) for binding single-stranded DNA is estimated to be between 6 and 12 nucleotides from kinetic studies (*12*), whereas structural data suggested the site size is minimally 5 nucleotides (*10*). If one assumes an average site size from these data of 8 nucleotides, it would be predicted that approximately 6−7 enzyme molecules would be sufficient to sequester the single-stranded DNA generated from F21:HF31. However, the stoichiometry for titration of F21 with E(wt) in the absence of Mg^{2+} was 1, which indicated that sequestration of F21 and HF31 formed from 1 mol of F21:HF31 would require at most 3 mol of E(wt). Thus, these considerations and the lack of ATP-independent strand separating activity of hE(V432A), which was deficient in ATP-independent strand-separating activity but competent in single-stranded DNA binding, suggested that the ATP-independent strand separating activity of E(wt) was more complicated than merely sequestering single-strand DNA as it was formed. However, it should be noted that the enzyme did not proceed with a given polarity in the ATP-independent strand-separating activity, whereas the enzyme proceeded with a 3′-polarity in the ATP-dependent helicase reaction. These findings bring into question whether the ATP-dependent and ATP-independent reactions are linked and suggest that polarity may be an ATP-dependent property of the enzyme. Nonetheless, an understanding of how multiple enzyme molecules couple their strand-separating potential into a single duplex such that strand separation is effected requires further study.

ACKNOWLEDGMENT

We acknowledge Steven Brown for instruction in the use of the response spectrophotometer for determining the T_m values of F21:HF31 and 21:31, E. Furfine for helpful discussions during the course of these studies, M. Rink for growing *E. coli* that expressed E(wt), Luke Carter for purifying hE(wt), and Walt Dallas and Dana Danger for cloning and construction of hE(wt) and hE(V432A) expression vectors.

REFERENCES

1. Matson, S. W., and Kaiser-Rogers, K. A. (1990) *Annu. Rev. Biochem. 59*, 289−329.
2. Lohman, T. M., and Bjornson, K. P. (1996) *Annu. Rev. Biochem. 65*, 169−214.
3. Choo, Q.-L., Kuo, G., Weiner, A. J., Overby, L. R., Bradley, D. W., and Houghton, M. (1989) *Science 244*, 359−362.
4. Choo, Q.-L., Richman, K. H., Han, J. H., Berger, K., Lee, C., Dong, C., Gallegos, C., Coit, D., Medina-Selby, A., Barr, P. J., Weiner, A. J., Bradley, D. W., Kuo, G., and Houghton, M. (1991) *Proc. Natl. Acad. Sci. U.S.A. 88*, 2451−2455.
5. Magrin, S., Craxi, A., Fabiona, C., Simonetti, R. G., Fiorentino, G., Marino, L., Diquattro, O., Di Marco, V., Loiacano, O., Volpes, R., Almasio, P., Urdea, M. S., Neuwald, P., Sanchez-Pescador, R., Detmer, J., Wilber, J. C., and Pagliaro, L. (1994) *Hepatology 19*, 273−279.
6. Abdel-Monem, M., and Hoffman-Berling, H. (1976) *Eur. J. Biochem. 65*, 441−449.
7. Subramanya, H. S., Bird, L. E., Brannigan, J. A., and Wigley, D. B. (1996) *Nature 384*, 379−383.
8. Yao, N., Hesson, T., Cable, M., Hong, Z., Kwong, A. D., Le, H. V., and Weber, P. C. (1997) *Nat. Struct. Biol. 4*, 463−467.
9. Korolev, S., Hsieh, J., Gauss, G. H., Lohman, T. M., and Waksman, G. (1997) *Cell 90*, 635−647.
10. Kim, J. L., Morgenstern, K. A., Griffith, J. P., Dwyer, M. D., Thomson, J. A., Murcho, M. A., Lin, C., and Caron, P. R. (1998) *Structure 6*, 89−100.
11. Bukh, J., Purcell, R. H., and Miller, R. H. (1994) *Proc. Natl. Acad. Sci. U.S.A. 91*, 8239−8243.
12. Preugschat, F., Averett, D. R., Clarke, B. E., and Porter, D. J. T. (1996) *J. Biol. Chem. 271*, 24449−24457.
13. Porter, D. J. T., Short, S. A., Hanlon, M. H., Preugschat, F., Wilson, J. E., Willard, D. H., Jr., and Consler, T. G. (1998) *J. Biol. Chem. 273*, 18906−18914.
14. Georgaki, A., Strack, B., Podust, V., and Hubscher, U. (1992) *FEBS Lett. 308*, 240−245.
15. Boehmer, P. E., and Lehman, I. R. (1993) *J. Virol. 67*, 711−715.
16. Chase, J. W., and Williams, K. R. (1986) *Annu. Rev. Biochem. 55*, 103−136.
17. Bjornson, K. P., Amaratunga, M., Moore, K. J. M., and Lohman, T. M. (1994) *Biochemistry 33* 14306−14316.
18. Gwack, Y., Kim, D. W., Han, J. H., and Choe, J. (1996) *Biochem. Biophys. Res. Commun. 225*, 654−659.
19. Suzich, J. A., Tamura, J. K., Palmer-Hill, F., Warrener, P., Grakoui, A., Rice, C. M., Feinstone, S. M., and Collett, M. S. (1993) *J. Virol. 67*, 6152−6158.
20. Matson, S. W., and George, J. W. (1987) *J. Biol. Chem. 262*, 2066−2076.
21. Taylor, A. F., and Smith, G. R. (1995) *J. Biol. Chem. 270*, 24451−24458.
22. Raney, K. D., Sowers, L. C., Millar, D. P., and Benkovic, S. J. (1994) *Proc. Natl. Acad. Sci. U.S.A. 91*, 6644−6648.
23. Preugschat, F., Dangar, D. P., Carter, L. H., III, Davis, R. G., and Porter, D. J. T. (2000) *Biochemistry 39*, 5174−5183.

BI992384F